Analysis of binding sites on complement factor I using artificial N-linked glycosylation.

Sánchez Gallego, José Ignacio; Groeneveld, Tom; Krentz, Stefanie; Nilsson, Sara; Villoutreix, Bruno O; Blom, Anna

Published in:
Journal of Biological Chemistry

DOI:
10.1074/jbc.M111.326298

2012

ANALYSIS OF BINDING SITES ON COMPLEMENT FACTOR I USING ARTIFICIAL N-LINKED GLYCOSYLATION*.

Jose I. Sanchez Gallego[1], Tom W.L. Groeneveld[1], Stefanie Krentz[1], Sara C. Nilsson[1], Bruno O. Villoutreix[2], and Anna M. Blom[1,a].

[1]Department of Laboratory Medicine, Medical Protein Chemistry, Malmö University Hospital, Lund University, Sweden; [2]INSERM U973 - MTi, University of Paris Diderot, Paris, France

Running title: *Structural investigation of complement factor I*

Address correspondence to: Anna Blom, Lund University; Dept. of Laboratory Medicine, Medical Protein Chemistry, University Hospital Malmö; S-205 02 Malmö, SWEDEN, Tel (+46) 40 33 82 33; Fax: (+46) 40 33 70 43, E-mail: Anna.Blom@med.lu.se

Keywords: Factor I, complement system, glycosylation.

Background: Artificial glycosylations were introduced to probe interactions of complement inhibitor Factor I (FI).
Results: Glycosylations in the FIMAC, CD5 and serine protease domains impaired FI function.
Conclusion: All analyzed cofactors form similar trimolecular complexes with FI and C3b/C4b.
Significance: Increased understanding of molecular mechanisms of complement inhibition.

ABSTRACT

Factor I (FI) is a serine protease that inhibits all complement pathways by degrading activated complement components C3b and C4b. FI functions only in the presence of several cofactors such as factor H, C4b-binding protein, complement receptor 1 and membrane cofactor protein. FI is composed of two chains linked by a disulphide bridge; the light chain comprises only the serine protease (SP) domain, while the heavy chain contains FI membrane attack complex domain (FIMAC), CD5 domain, low-density lipoprotein receptor 1 (LDLr1) and LDLr2 domains. To better understand how FI inhibits complement, we used homology-based 3D models of FI domains in an attempt to identify potential protein-protein interaction sites. Specific amino acids were then mutated to yield 20 recombinant mutants of FI carrying additional surface exposed N-glycosylation sites that were expected to sterically hinder interactions. The Michaelis constant (K_m) of all FI mutants toward a small substrate was not increased. We found that many mutations in the FIMAC and SP domains nearly abolished ability of FI to degrade C4b and C3b in the fluid phase and on the surface, irrespectively of the cofactor used. In the other hand only few alterations in the CD5 and LDLr1/2 domains impaired this activity. In conclusion, all analyzed cofactors form similar trimolecular complexes with FI and C3b/C4b, and the accessibility of FIMAC and SP domains is crucial for the function of FI.

INTRODUCTION

The complement system is a key component of the innate immune system. Proper activation and regulation of complement are crucial to protect self-tissues from damage (1). The main functions of complement are defense against infections, clearance of immune complexes and apoptotic cells and alerting the adaptive immune system. When triggered by a pathogen or danger associated patterns, complement is activated via a cascade of proteolytic cleavages organized in the classical, lectin and alternative pathways.

To prevent spontaneous complement activation that could lead to systemic depletion, as well as to regulate activation by self-tissue, complement is controlled by both fluid-phase and membrane bound inhibitors (2). Factor I (FI) (3) is a key serine protease that inactivates all complement pathways by degrading activated complement factors C3b and C4b, but exclusively in the presence of cofactors such as factor H (FH) (4), C4b-binding protein (C4BP) (5), membrane cofactor protein (MCP)

(6) and complement receptor 1 (CR1) (7). A complete FI deficiency results in an uncontrolled activation of the amplification loop of the alternative pathway, leading to the consumption and depletion of C3. This in turn leads to a defect in opsonization, immune adherence and phagocytosis (8). Heterozygous mutations in FI have been also identified in patients with atypical hemolytic uremic syndrome (aHUS) (9-12).

FI is a multidomain acute-phase glycoprotein (88 kDa) that circulates in the blood at concentration of 35 μg/ml (13). FI is produced mainly in the liver, but also by monocytes (14), fibroblasts (15), keratinocytes (16) and endothelial cells (17). It is synthesized as a single polypeptide chain of 66 kDa and N-glycosylated at six positions (25-27% w/w) with heavily sialylated biantennary glycans (18). It is then proteolytically processed into the heavy (50 kDa) and the light chain (38 kDa) that remain covalently linked by a disulfide bond (19,20). The heavy chain is composed of five domains: FI-membrane attack domain (FIMAC), the CD5-like domain (CD5) also known as a scavenger receptor cysteine-rich (SRCR) domain, the low lipoprotein receptor 1 and 2 (LDLr1 and 2) and a small region of unknown homology. The light chain comprises the serine protease domain (SP), which contains the catalytic triad His-362, Asp-411 and Ser-507. Among the 40 cysteines present in the FI molecule, four of them connect separate domains, the FIMAC with the LDLr1 domain, and the SP domain with the heavy chain. The remaining cysteines are all paired in intradomain disulphide bonds. Low-resolution 3D-structure of FI was studied by both x-ray neutron scattering and electron microscopy (21,22) and recently a high-resolution structure was obtained by X-ray spectroscopy (23).

FI circulates in a zymogen-like state in blood (23) and does not have any known physiological inhibitor, although synthetic inhibitors such as suramin are able to weakly inhibit it (24). This together with the fact that FI is probably maintained in its inactive form by the allosterically modulating activity of the non-catalytic heavy chain on the light chain (23), suggests that the active site of FI is hidden or conformationally altered by the heavy chain and only becomes exposed when its substrates or cofactors are bound (22).

In spite of all the accumulated knowledge about the function and structure of the FI molecule, it is currently still not known how exactly FI interacts on the molecular level with either its substrates or co-factors. We previously developed homology-based models of the individual domains of FI (25), which we used to identify some of the functionally important amino acids in the heavy chain of FI (26). These models were used in the current study to design novel N-glycosylation sites at the putative binding areas on the whole FI. These surface exposed glycosylations were expected to sterically hinder interactions of FI with its ligands while introducing little perturbations in the structure of FI. Functional analyses carried out with purified FI mutants showed that FIMAC, CD5 and SP domains are important in the interaction between the enzyme and its substrates, in the presence of different cofactors, in order to degrade C3b and C4b in the fluid-phase as well as C3b deposited on the surface of cells. These data help to understand the importance and function of the different domains of FI in its interaction with other proteins.

EXPERIMENTAL PROCEDURES

Design of additional N-linked glycosylations using homology-based 3D model of FI - The 3D models of the different domains of human FI were described previously (12,25). The numbering of the amino acid residues in FI used in this study is based on the mature protein without signal sequence. Interactive structural analysis of the models guided us to select a limited number of surface areas to assess experimentally. The residues that were targets for the addition of extra N-glycans by mutagenesis were solvent-exposed and not involved in any clear stabilizing interactions with the remaining parts of each domain (e.g., salt bridges) and the amino acid substitutions were, therefore, expected to be well tolerated. In each case one or more amino acids were mutated in order to form consensus sequence for addition of N-linked carbohydrates (N-X-S/T) (Fig. 1A, C)

Proteins - Human C4BP (27) and FH (28) were purified as described previously. C1, C2, C3, C3b, C4, C4b, factor B (FB) and factor D (FD) were purchased from Complement Technology (Tyler, TX). C3b and C4b were labeled with ^{125}I using the chloramine T method as described (29). C3met and C4met

were prepared by treatment with methylamine. C3 and C4 were incubated with 100 mM methylamine, pH 8.0, at 37°C for 1 h to hydrolyze the internal thioesther bond. C3met and C4met were then dialyzed overnight in 50 mM Tris-HCl, 150 mM NaCl, pH 8.0, at 4°C. C3met/C4met still retain the anaphylatoxin domain but resemble C3b/C4b in overall conformation and properties.

FI cDNA Clones for Recombinant Proteins - Eukaryotic expression vector pcDNA3 (Invitrogen) containing human FI cDNA with addition of an N-terminal His Tag after signal sequence (11) was used. The mutations were introduced in the FI cDNA using primers listed in Table 1 and the QuickChange site-directed mutagenesis kit (Stratagene, La Jolla, CA). The mutations were confirmed by automated DNA sequencing using the Big dye terminator kit (Applied Biosystem, Foster City, CA).

Purification of Recombinant FI - FI and wt mutants were expressed in a stable manner in human embryonic kidney (HEK 293) cells and purified from conditioned media (Optimem, Invitrogen) by affinity chromatography using nickel-nitriloacetic and Superflow resin (Qiagen, Hilden, Germany) as described (25). The purified recombinant FI mutants were visualized using goat antibodies (Quidel, San Diego, CA) on Western blot as described (25). All proteins were stored at -80°C. Protein concentrations were determined by measuring the absorbance at 280 nm and subtracting the absorbance at 320 nm. The concentrations were then verified by SDS/PAGE electrophoresis followed by Coomassie staining of proteins.

Amidolytic Assay - The amidolytic assay was essentially performed as described (24). Briefly, wt FI or the individual mutants, at a final concentration of 25 μg/ml, were combined with different concentrations (200, 100, 25, 6.25 mM final concentration) of DPR-AMC substrate (*t*-butoxycarbonyl-Asp(benzyl)-Pro-Arg-amidomethylcoumarin-HCl; Bachem Bubendorf, Switzerland) in Bicine buffer (25 mM Bicine, 0.5 mM EDTA, 146 mM NaCl, H_2O, pH 8.25). These were transferred to black optical plates (Nunc, Roskilde, Denmark), and the activity of each enzyme was subsequently determined using a microplate reader (Tecan infinite 200, Tecan, Männerdof, Switzerland) with excitation at 360 nm and an emission readout at 465 nm for 1 h at 37°C. Using Graphpad Prism 5.0 (Graphpad Software, La Jolla, CA), both maximum initial velocity (V_{max}) and the Michaelis constant (K_m) of all enzymes were calculated using nonlinear regression analysis. The amount of substrate converted in the reaction was calculated from the fluorescence units using a conversion factor, which was determined from complete substrate turnover using thrombin as a converting enzyme.

C4b and C3b Degradation Assay - To assay degradation of C4b, recombinant FI wt or mutant proteins were diluted to a final concentration of 1, 2.5, 5 or 10 μg/ml and mixed with 100 μg/ml C4BP, 50 μg/ml C4met, and trace amounts of ^{125}I-labeled C4b. The positive control contained 100 μg/ml C4BP and 20 μg/ml wt FI, whereas in the negative control FI was omitted. The C3b degradation assay was similar except that 20 μg/ml FH, 150 μg/ml C3met, 1, 2.5, 5 or 10 μg/ml of FI, and trace amounts of ^{125}I-labeled C3b were incubated together. To determine FI activity in the presence of CR1 as a cofactor, human erythrocyte ghosts were prepared as described previously (30) and added as a source of CR1. Two concentrations of FI were tested: 1 and 10 μg/ml and incubated with 150 μg/ml C3b and trace amounts of ^{125}I-labeled C3b. We further used lung cancer cell line H2087 as a source of the cofactor MCP, a cell line that we have previously shown to express MCP but no CR1 (31). The H2087 were harvested with versene (Invitrogen) and solubilized at 8 x 10^7 cells/ml in phosphate-buffered saline containing 1% Nonidet P-40 and 2 mM phenylmethylsulfonyl fluoride. After centrifugation (25,000 rpm, 30 min, 4°C), 3 μl of clear cell extract was added to 1, 5 or 10 μg/ml of FI together with 150 μg/ml C3b and trace amounts of ^{125}I-labeled C3b. Irrespective of the cofactor, in all assays where degradation of C3b was tested, 20 μg/ml FI and 20 μg/ml FH were used as a positive control, whereas in the negative controls FI was omitted. In all reactions the samples were incubated at 37°C for 90 min, and the reactions were stopped by adding reduced sample buffer and boiling for 3 min. The proteins were separated on a 10-15% gradient SDS-PAGE gel and visualized using a Fluorescent image analyzer (Fujifilm, Tokyo, Japan). The intensity of the cleavage products (C4d and 43 kDa) of C4b and C3b were analyzed using ImageGauge software

(Fujifilm). Each experiment was repeated three times.

Degradation of surface-bound C3b by FI - C3b was deposited on sheep erythrocytes by incubation with C3, FB and FD as described (11). This was followed by incubation with 20 μg/ml FH and 0.1, 0.5 and 1 μg/ml recombinant wt or mutant FI at 37°C for 60 min. After washing, iC3b and C3d were detected using mouse monoclonal anti-human iC3b and anti-human C3d antibodies, respectively (both at 5 μg/ml, Quidel) followed by goat anti-mouse antibodies conjugated to fluorescein isothiocyanate (diluted 1:100, Dako) and analyzed by flow cytometry (Partec, Germany, Münster). The experiment was repeated three times, and the results were analyzed using FlowJo software (Three Star, Ashland, OR).

Deglycosylation Assay - Mutants were deglycosylated using the Native Protein Deglycosylation kit (Sigma Aldrich). For this purpose wt and the mutants characterized to have impaired function (125 and 62.5 μg/ml) were incubated for 24 h at 37°C in the presence or absence of three different endoglycosidases with a ratio enzyme:glycoprotein 0.03 (v/w). Subsequently, all the samples were analyzed using a C3b degradation assay using FH as cofactor and 20 μg/ml of FI as a positive control, as described above. The intensity of the cleavage product (43 kDa) of C3b was analyzed using ImageGauge software (Fujifilm). Each experiment was repeated six times.

Direct binding of FI to C3met/C4met - Microtiter plates (Maxisorp, Nunc) were coated with C3met/C4met (5 μg/ml) in 50 mM sodium carbonate buffer, pH 9.6, overnight at 4°C. The wells were blocked with 1% bovine serum albumin (BSA) in phosphate-buffered saline for 2 h at room temperature, and then wt and mutant FI, 100 μg/ml diluted in 0.5X phosphate-buffered saline containing 1% BSA and 0.05% Tween 20, were added to the wells for 1h at 37°C. The same buffer was used for washing at each step. The binding of FI to C3met/C4met was detected using goat-anti-FI antibodies (Quidel) followed by horseradish peroxidase-labeled rabbit-anti-goat antibodies (Dako) and the OPD development kit (Dako). The absorbance was measured at 490 nm, and the values obtained for each mutant without C3met/C4met coating (1% BSA) and those with only FI omitted were subtracted as background. Each experiment was repeated three times in duplicate.

Statistical Methods - One-way ANOVA with Tukey's multiple comparison tests and Two-way ANOVA with Bonferroni post-tests were performed using GraphPad Prism to assess the statistical significance of observed differences.

RESULTS

Expression and characterization of wt FI and mutant proteins - In our previous study we have shown using site directed mutagenesis that several solvent-exposed amino acids in FIMAC and CD5 domains of FI were important for its function (26). Now we used a different approach to screen most of the surface of FI for potential binding sites. To this end, we have introduced 20 additional N-glycosylation sites in FI (Fig 1A). The mutants were designed using the 3D structure of the individual domains built by homology. As the X-ray structure of FI had just became available (23), each model was superimposed on the experimental structure (Fig. 1B). The rmsd for the C-alpha between the model and the X-ray is 1.7 Å for the FIMAC, 2.3 Å for the CD5-like, 0.6 Å for the LDLr1, 0.7 for the LDLr2, 1.1 Å for the SP domain, indicating that the models were overall accurate. The two Ca^{2+} binding sites could be located in the model and are also visible in the experimental structure. To assess how the addition of these extra N-glycans affected the functional activity of FI the wt and mutant FI constructs were transfected in HEK 293 cells in a stable manner. Twenty mutants were successfully expressed, purified by affinity chromatography and visualized using Western blotting (Fig. 2). All mutants migrated as slightly larger proteins compared to wt FI, both under non-reducing (Fig. 2) and reducing conditions (not shown). The observed increase in apparent mobility suggests the presence of an additional N-linked glycan in each mutant.

Enzymatic Activity of FI mutants - To confirm that the FI mutants retained the catalytic triad in a functional conformation, their enzymatic activity towards a small substrate (t-butoxycarbonyl-Asp(benzyl)-Pro-Arg-amidomethylcoumarin; DPR-AMC) was compared with the wt control in an amidolytic assay. This assay measures the enzymatic activity that is independent of cofactors. None of the mutants showed a statistically

significantly lower V_{max} or higher K_m value compared to the wt indicating that enzymatic activity was not decreased by the introduced mutations (Table 2). Interestingly, some of the mutants showed a significant decrease in the K_m value compared to wt FI, suggesting a greater affinity for the small substrate DPR-AMC.

Mutations in the FIMAC, CD5 and SP domains of FI caused impaired degradation of C3b and C4b in fluid-phase - In order to find out whether the mutations affect the function of FI, fluid-phase degradation assay of C3b and C4b were performed. Different concentrations of the wt or mutant FI were incubated with fluid-phase cofactors (FH or C4BP) and ^{125}I-labeled C3b/C4b and then analyzed by SDS-PAGE (only 10 μg/ml concentration is shown). In the representative gel picture (Fig. 3A), where 10 μg/ml FI was used, the negative control shows intact bands for the α' and β chains of C3b, whereas in the positive control the α' was degraded and the 68-, 46- and 43-kDa products generated. Intensities of bands corresponding to the 43-kDa products were calculated from three independent gels, and the obtained mean value was related to the positive control (Fig. 3B). In the gel picture of C4b (10 μg/ml FI), the negative control shows intact bands for α', β and γ chains, and the positive control shows that α' chain is degraded while C4d is generated (Fig. 3C). Intensities of bands corresponding to the C4d product were calculated from three different gels, and the obtained mean value related to the positive control and presented in Fig. 3D. Three out of four mutations introduced in the FIMAC domain resulted in impaired or near complete loss of activity of FI in degradation of both C3b and C4b in the presence of FH and C4BP, respectively. The R61N mutant is the exception in this FIMAC domain, preserving totally the proteolytic activity of the enzyme in the fluid phase. In the CD5 domain the mutant L171N caused the total loss of activity of FI in the presence of both fluid-phase cofactors. None of the mutants in LDLr1 and LDLr2 domains impaired the normal activity of the enzyme, although when C4BP was used as cofactor, the mutant Q242N/K244S (LDLr2 domain) had statistically lower activity than the wt. All of the mutations in the SP domain diminished the degradation capacity of C3b and C4b by FI, except the mutants N404T and D420N/N422T in the presence of FH, which showed no differences compared to wt.

To investigate if the differences in the activity of the mutants depend on the cofactor used, we also performed the degradation assay of C3b using MCP and CR1 as FI cofactors. As positive control we used 20 μg/ml FI and 20 μg/ml FH, while the negative control lacked FI. Different concentrations of mutants or wt were incubated with MCP or CR1 and ^{125}I-C3b and then analyzed by SDS-PAGE (only 20 μg/ml concentration is shown) (Fig. 4A, C). The intensities of the 43-kDa product bands were calculated from independent experiments and the mean values of the positive control are shown for MCP (Fig. 4B) and CR1 (Fig. 4D). The results obtained were quite similar to those using FH and C4BP as cofactors. The mutations in FIMAC led to the complete loss of enzymatic activity, except for the mutant R61N that preserved the same activity as wt. In the CD5 domain, the mutant L171N showed almost no activity, while the rest of mutations had no impact on the ability of FI in degrading C3b in fluid-phase. The mutants Q242N/K244S and Q257N/Q259S had statistically significantly lower activity than wt and seemed to affect slightly the activity of FI when CR1 was used as cofactor, compared to the activity of the enzyme in the presence of FH or C4BP. All the mutations in the SP domain impaired partially or totally the normal function of FI. Taken together, we can conclude that the analyzed mutations affect the activity of FI in a similar manner, independently of the cofactor used.

FI degradation of surface-bound C3b - To test if the addition of an extra N-glycan causes a different effect when FI is degrading a substrate on a surface as opposed to the fluid phase, we analyzed all the mutants with a degradation assay of C3b deposited on sheep erythrocytes using flow cytometry. Erythrocytes opsonized with C3b were incubated with FI and FH, and the cleavage products, iC3b and C3d, were detected with specific antibodies. The higher the ratio iC3b:C3d the more degradation of C3b by FI. The results obtained were essentially similar to those found in degradation assays in fluid-phase (Fig. 5). The FIMAC domain was again the most affected by mutations, as impaired or near complete loss of activity of all mutants except for R61N that showed high activity was

observed. In the CD5 domain three out of four of the mutants retained almost the same activity as wt, but the presence of a new glycan in the L171N mutant impaired completely the activity of the enzyme. Most of the mutations in the LDLr1 and 2 domains did not affect the enzymatic activity with the exception of the mutant Q219N/K221S that had lower activity in one of the concentrations tested. The SP domain was very sensitive to the addition of a glycan, resulting in an impaired degradation activity in half of the mutants, and a completely loss of activity in the other half. Only the N404T mutant retained its proteolytic activity when compared to wt.

Restored activity after deglycosylation - To analyse whether those mutants that were partially or totally impaired could recover their activity after deglycosylation, they were digested with endoglycosidases under native conditions. As a negative control, each mutant was also incubated in the absence of the endoglycosidases. After the treatment, which resulted in at least partial deglycosylation as determined by SDS/PAGE (not shown), a fluid-phase degradation assay of C3b using FH as cofactor was performed (Fig. 6). The ability of wt FI to degrade C3b was not affected by the treatment with endoglycosidases, showing that the removal of the six naturally occurring glycans on FI did not affect the ability to degrade C3b. Of the six mutants that were almost totally impaired in their function three recovered their activity significantly after being deglycosylated, two in the FIMAC domain (R35N/I37T, F82N/N84T) and one in the SP domain (S561N/Y563T). The rest of the mutants did not reveal significant differences in their activities after deglycosylation.

Binding of wt and mutant FI to C3met or C4met - To elucidate if the reduced function of some mutants could be caused by impaired binding to C3b or C4b, a direct binding assay was performed. Wt and mutant FI were allowed to bind to C3met- or C4met-coated microtiter plates, and the binding was detected with antibodies against FI (Fig. 7). The background values were subtracted and the results were normalized against wt FI. This was necessary because the interaction between C3b and FI is difficult to detect due to low affinity. Mutations in the FIMAC, CD5 and LDLr1 domains did not decrease the binding of the enzyme to C3met or C4met. On the contrary, some mutants appeared to bind stronger than the wt to C3met (T54N/V56T, F82N/N84T, L171N) and C4met (T54N/V56T, K124N, L171N). FI was significantly impaired in its binding to C4met due to Q242N/K244S, Q257N/Q259S mutations in LDLr2, and the R365N and N404T mutations in the SP domain. The results for mutations in these domains for C3met were similar but with two more mutations in SP that showed impaired binding (K326N/A328T and D420N/N422T).

DISCUSSION

The normal function of complement depends on a tight balance between activation and inhibition of the components. Therefore, FI has a crucial physiological function inactivating all complement pathways by degrading C3b and C4b in the presence of a cofactor. With this study we continue the line of research about relationships between structure and function of FI. In a previous study (26) we have investigated 18 FI mutants with amino acid changes only in the heavy chain and found that mainly alterations in the FIMAC domain had an effect on function of FI. However, these mutations were analyzed only in the context of the individual FI domains as it was at that time not possible to predict the overall structural organization of the whole FI. In the current study we have used a different strategy to further probe the surface of FI by introducing N-glycosylation both in the heavy and the light chain of FI. Glycosylation generally induces a more pronounced effect than amino-acid change and thus these two approaches complement each other. Furthermore, the effects of the introduced glycosylations were now interpreted using combined models and recently published X-ray structure of FI (23).

The molecular events leading to the cleavage of C3b/C4b by FI in the presence of cofactors are not well established at present. It has been shown that even in the absence of any cofactors FI is able to weakly interact with C3b, which induces a conformational change in the enzyme (32). This binding was demonstrated to be dependent on ionic interactions between amino acids (20). It has also been demonstrated, using x-ray crystallography, that the binding of FH to C3b leads to a conformational change in the latter resulting in the accessibility of peptide bonds that can be cleaved by FI (33). The SP domain

in the light chain of FI contains the catalytically active site, which is able to degrade activated complement components *in vivo* but only in the presence of a cofactor. However, the SP domain is also able to degrade small synthetic amide substrates in the absence of any cofactor (24). Furthermore, the isolated SP domain prepared by limited proteolytic degradation of FI slowly cleaved C3b in the absence of any cofactor and did so at more than the usual two sites. This suggests that perhaps the heavy chain performs the function of blocking or maintaining the SP domain in an inactive conformation. Moreover, the cofactors and probably the SP domain may be important in orienting the natural substrates in such a way as to restrict the cleavage to a few specific sites leading to well defined degradation products. Despite being heavily glycosylated, native and deglycosylated FI have similar proteolytic activities against C3 (18) implying that the naturally occurring glycosylation are not involved in orienting FI in relation to substrate and cofactor. Accordingly, all natural glycosylations are essentially present on the face of the FI molecule pointing away from FH and C3b in the model of the complex (Fig 1C, inset).

The goal of the current study was to explore potential protein-protein binding sites on the surface of both the light and the heavy chains of FI. The 3D structures of the different domains of FI were predicted using homology modeling (26) and used to identify the key solvent exposed regions where a glycosylation site could be created allowing to probe most of the surface with a minimum number of mutations. Very recently, the crystal structure of FI was solved (23) allowing us to refine further the interpretation of our results. As several regions of the FI experimental X-ray structure were not defined, we superimposed our homology models onto the corresponding domains of the experimental structure (Fig. 1B). The different domains were predicted accurately by modeling but we lacked the overall organization of the protein, which was now possible to construct using the experimental structure. The majority of the newly introduced glycosylation sites were solvent exposed in the experimental FI structure except for residue 82 (see below), and for residue 171 in the CD5 domain located essentially at the interface with the FIMAC domain. To investigate further the possible functional impact of the introduced mutations, we built a model of the FI-FH-C3b complex following the previously described procedure (23) (Fig. 1 C, inset).

A glycosylation at residue 35 in the FIMAC domain, which impairs FI activity in our experiments, could act on the binding of FH or by modifying the FI intra domain contacts, as the new sugar side chain would point toward the SP domain and it is not far from FH. The function of the R35N/I37T mutant could be largely restored upon deglycosylation. The glycosylation at position 54 (which showed impaired activity in the degradation of C3b or C4b) is positioned away from the expected binding region for FH and C3b in our model of the complex. However a glycosylation at this site could modify the orientation of the FI domains, possibly by changing the orientation of the CD5 domain, which could in turn affect the interaction with FH. The mutation at this site, in the absence of glycosylation, is unlikely to modify the function of FI as there is no interaction with the other domains of FI. Surprisingly, the reduced activity of T54N/V56T mutant was not restored after deglycosylation. This is likely due to the fact that complete deglycosylation at this site under native conditions was not fully obtained. The mutant involving residue 61 functioned as wt FI with regard to C3b or C4b degradation in fluid-phase. As this residue points away from all FI domains and the FH-C3b complex, a glycosylation at this site is compatible with the observed experimental data. The mutation and/or the glycosylation at position 82 is likely to disturb the local folding of the FIMAC domain and this in turn affects the function of FI, in agreement with the strong impaired activity seen in the functional assays. This structural problem could in turn affect FH binding since the cofactor is at about 9 Å from the mutation in our model of the complex. In fact, in our initial homology model, the side chain of Phe 82 was essentially solvent exposed, while in the X-ray structure it is essentially buried inside the domain. The inaccurate modeling of amino acid side chains in insertion/deletion regions is well known in comparative modeling. For this residue the prediction was not correct and therefore mutation should not have been planned. However, there was a partial but statistically significant recovery in the activity of this

mutant after deglycosylation indicating that the presence of an extra glycan in this area might be responsible for the impaired function of the enzyme. Taken together, the current results are in good agreement with our previously published data on series of point mutations introduced in the FIMAC domain (26) and together support the hypothesis that the FIMAC domain is involved in multiple interactions crucial for the function of FI. Initially one could have hypothesized that the FIMAC directly occludes the active site on the SP domain particularly since it adopts a fold commonly found in serine protease inhibitors. However, the crystallographic structure showed that the active site is exposed and that the FIMAC domain most likely acts on the SP domain by inducing structural changes (23). The preliminary model of the complex, built following the reported data (23) together with our analysis suggest that one face of the FIMAC domain is likely to be close to FH, thereby shedding some new insights on the complex molecular mechanisms that are taking place in this biological system.

Analysis of mutations at positions 104 and 124 in the CD5 domain shows that both these regions are fully exposed in our model of the FI-C3b-FH complex suggesting that they should not affect the ability of FI to degrade C4b or C3b, which is in agreement with our experimental data. Glycosylation at position 171 most likely disturbs the FI intra domain contacts as it is located at the interface with the FIMAC and LDLr1 and thus impedes the degradation of C3b or C4b. It would seem that this region could tolerate the L to N substitution without creating folding problems as the Leu residue is next to polar amino acids (Q31, H22, R169, Q232) in the X-ray structure of FI. The results obtained in the deglycosylation assay showed no recovery in the activity of this mutant but this is likely due to incomplete deglycosylation because this residue is in part buried between the domains. The improved binding to C3met is likely due to structural changes that propagate to the binding site of C3b. Glycosylation at position 182 should put the sugar chain far away from C3b-FH and this residue is not in contact with the other domains of FI and thus the structural analysis is in line with the observed wt-like function of the mutated FI *in vitro*.

Structural analysis of the mutations in the LDLr domains suggests that a sugar side chain at position 242 (LDLr2) could modify the function of FI by slightly re-orienting the CD5 domain or the LDLr1 thereby impeding normal binding to C3b. This is in good agreement with the experimental data as binding to C3met is impaired. This holds true also for the mutation at the residue 257. Surprisingly, glycosylation at the position 210 does not affect binding to C3met nor the function of FI while it would appear to point in the direction of C3b in our model of the complex. It is possible that the sugar side chain does not contact the substrate. Alternatively, this may suggest that the positioning of FI on the C3b-FH surface needs to be modified in this area.

Analysis of the SP domain shows that all newly introduced glycosylations point away from the other domains of FI and therefore should not affect the overall structure of FI. S561, D402, R365, D497 and K458 are close to the C3b-FH structures in the model of the complex, which is in good agreement with experimental data showing that all these mutations decreased FI activity in degradation of C3b and C4b. Glycosylations at position 365 and 402 affected binding of FI to C3b. These amino acid substitutions, in the absence of efficient glycosylation could also have this effect as these areas of the SP domain point toward C3b in the model of the complex. The 326, 385, 420 residues are away from C3b-FH and thus could affect FI through allosteric mechanisms or through stabilization, which could result in lower binding to C3b as found for glycosylations at residues 326 and 420. The deglycosylation of FI, particularly the SP domain, under native conditions was difficult. In the SP domain only one out of six mutants (S561N/Y563T) was successfully deglycosylated, recovering significantly its activity. As mentioned before, we cannot exclude the effect of the mutations themselves in the impairment of the activity of the enzyme. However, the results of the amidolytic assay indicate that all mutants retained or increased the enzymatic activity towards the DPR-AMC substrate. This shows that the mutations themselves did not lead to a detrimental change of conformation in the catalytic triad. Western blot analysis after deglycosylation revealed partial deglycosylation of wt and all mutants but complete deglycosylation was not achieved even after very prolonged incubation times (not shown).

In general, the effects of the introduced glycans on the activity of FI were similar in most cases irrespectively of which cofactor proteins were used in the assay. This implies that the general structure of the trimolecular complex between FI, C3b/C4b and any of the tested cofactors is similar to one another. In agreement with this hypothesis we found that mutations in FI that affected binding of FI to C3b also impaired interaction with C4b. Glycosylation of residue 402 impaired the activity of FI when C4BP, MCP and CR1 were used but not FH. These results show that there still are small differences in the positioning of some regions of the cofactors-substrate on the surface of FI and thus that some binding sites do not overlap completely. The data also suggest that the very preliminary model of the complex (23) could be correct, although the interactions will have to be probed further to refine our atomic understanding of the contacts.

REFERENCES

1. Ricklin, D., Hajishengallis, G., Yang, K., and Lambris, J. D. (2010) *Nat Immunol* **11**, 785-797
2. Sjoberg, A. P., Trouw, L. A., and Blom, A. M. (2009) *Trends Immunol* **30**, 83-90
3. Nilsson, S. C., Sim, R. B., Lea, S. M., Fremeaux-Bacchi, V., and Blom, A. M. (2011) *Mol Immunol* **48**, 1611-1620
4. Weiler, J. M., Daha, M. R., Austen, K. F., and Fearon, D. T. (1976) *Proc Natl Acad Sci U S A* **73**, 3268-3272
5. Gigli, I., Fujita, T., and Nussenzweig, V. (1979) *Proc Natl Acad Sci U S A* **76**, 6596-6600
6. Seya, T., Turner, J. R., and Atkinson, J. P. (1986) *J Exp Med* **163**, 837-855
7. Medof, M. E., and Nussenzweig, V. (1984) *J Exp Med* **159**, 1669-1685
8. Sunyer, J. O., Zarkadis, I. K., and Lambris, J. D. (1998) *Immunol Today* **19**, 519-523
9. Fremeaux-Bacchi, V., Dragon-Durey, M. A., Blouin, J., Vigneau, C., Kuypers, D., Boudailliez, B., Loirat, C., Rondeau, E., and Fridman, W. H. (2004) *J Med Genet* **41**, e84
10. Kavanagh, D., Richards, A., Noris, M., Hauhart, R., Liszewski, M. K., Karpman, D., Goodship, J. A., Fremeaux-Bacchi, V., Remuzzi, G., Goodship, T. H., and Atkinson, J. P. (2008) *Mol Immunol* **45**, 95-105
11. Nilsson, S. C., Karpman, D., Vaziri-Sani, F., Kristoffersson, A. C., Salomon, R., Provot, F., Fremeaux-Bacchi, V., Trouw, L. A., and Blom, A. M. (2007) *Mol Immunol* **44**, 1835-1844
12. Nilsson, S. C., Kalchishkova, N., Trouw, L. A., Fremeaux-Bacchi, V., Villoutreix, B. O., and Blom, A. M. (2010) *Eur J Immunol* **40**, 172-185
13. Catterall, C. F., Lyons, A., Sim, R. B., Day, A. J., and Harris, T. J. (1987) *Biochem J* **242**, 849-856
14. Whaley, K. (1980) *J Exp Med* **151**, 501-516
15. Vyse, T. J., Morley, B. J., Bartok, I., Theodoridis, E. L., Davies, K. A., Webster, A. D., and Walport, M. J. (1996) *J Clin Invest* **97**, 925-933
16. Timar, K. K., Junnikkala, S., Dallos, A., Jarva, H., Bhuiyan, Z. A., Meri, S., Bos, J. D., and Asghar, S. S. (2007) *Mol Immunol* **44**, 2943-2949
17. Julen, N., Dauchel, H., Lemercier, C., Sim, R. B., Fontaine, M., and Ripoche, J. (1992) *Eur J Immunol* **22**, 213-217
18. Tsiftsoglou, S. A., Arnold, J. N., Roversi, P., Crispin, M. D., Radcliffe, C., Lea, S. M., Dwek, R. A., Rudd, P. M., and Sim, R. B. (2006) *Biochim Biophys Acta* **1764**, 1757-1766
19. Goldberger, G., Arnaout, M. A., Aden, D., Kay, R., Rits, M., and Colten, H. R. (1984) *J Biol Chem* **259**, 6492-6497
20. Fearon, D. T. (1977) *J Immunol* **119**, 1248-1252
21. Perkins, S. J., Smith, K. F., and Sim, R. B. (1993) *Biochem J* **295 (Pt 1)**, 101-108
22. DiScipio, R. G. (1992) *J Immunol* **149**, 2592-2599
23. Roversi, P., Johnson, S., Caesar, J. J., McLean, F., Leath, K. J., Tsiftsoglou, S. A., Morgan, B. P., Harris, C. L., Sim, R. B., and Lea, S. M. (2011) *Proc Natl Acad Sci U S A* **108**, 12839-12844
24. Tsiftsoglou, S. A., and Sim, R. B. (2004) *J Immunol* **173**, 367-375
25. Nilsson, S. C., Trouw, L. A., Renault, N., Miteva, M. A., Genel, F., Zelazko, M., Marquart, H., Muller, K., Sjoholm, A. G., Truedsson, L., Villoutreix, B. O., and Blom, A. M. (2009) *Eur J Immunol* **39**, 310-323

26. Nilsson, S. C., Nita, I., Mansson, L., Groeneveld, T. W., Trouw, L. A., Villoutreix, B. O., and Blom, A. M. (2010) *J Biol Chem* **285**, 6235-6245
27. Dahlback, B., Nilsson, I. M., and Frohm, B. (1983) *Blood* **62**, 218-225
28. Blom, A. M., Kask, L., and Dahlback, B. (2003) *Mol Immunol* **39**, 547-556
29. Greenwood, F. C., Hunter, W. M., and Glover, J. S. (1963) *Biochem J* **89**, 114-123
30. Spiller, O. B., Blackbourn, D. J., Mark, L., Proctor, D. G., and Blom, A. M. (2003) *J Biol Chem* **278**, 9283-9289
31. Okroj, M., Hsu, Y. F., Ajona, D., Pio, R., and Blom, A. M. (2008) *Mol Immunol* **45**, 169-179
32. Ekdahl, K. N., Nilsson, U. R., and Nilsson, B. (1990) *J Immunol* **144**, 4269-4274
33. Wu, J., Wu, Y. Q., Ricklin, D., Janssen, B. J., Lambris, J. D., and Gros, P. (2009) *Nat Immunol* **10**, 728-733

FOOTNOTES

* This work was supported Swedish Research Council (K2009-68X-14928-06-3), the Söderberg Foundation, Swedish Foundation for Strategic Research and Foundations of Österlund, Greta and Johan Kock, Knut and Alice Wallenberg and Inga-Britt and Arne Lundberg. The authors declare no financial conflict of interest.

The abbreviations used are: aHUS, atypical hemolytic uremic syndrome; BSA, bovine serum albumin; C4BP, C4b-binding protein; CR1, complement receptor 1; DFP, diisopropylfluorophosphate; FB, factor; FD, factor D; FH, factor H; FI, factor I; FIMAC, factor I membrane attack complex (domain); LDLr, low density lipoprotein receptor; MCP, membrane cofactor protein; NHS, normal human serum; SP, serine protease (domain)

FIGURE LEGENDS

FIGURE 1. Three-dimensional overview of the glycosylation sites. A. Mutations on the schematic diagram of FI. FI is composed of the following domains: FIMAC, CD5-like, LDLr1 and LDLr2, a small region of unknown homology and the SP (serine protease) domain. The positions of natural N-linked glycosylation are marked with arrows, and two important interdomain disulfide bridges are indicated. The mutations are numbered without the signal peptide. B. Predicted 3D structure of the individual domains of FI superimposed onto the X-ray structure of FI (grey) (23). FI is displayed as follows: the FIMAC domain (blue), the CD5-like (green), the LDLr1 (yellow) and LDLr2 (orange), a small region of unknown homology (grey helix in the X-ray structure) and a SP domain (red). C. The constructed glycosylation sites. The mutations (amino acid changes to form consensus sequence (N-X-S/T)) are shown as CPK spheres (blue). Six natural N-glycans are shown in olive and the Asn residue number is boxed. The labels of the inserted N-glycans are colored in dark blue (when they do not or only slightly affect FI activity) and in black and underlined (when they cause significant impairment of FI activity). The figure was prepared with PyMol. Inset: Putative model of the FI-fH-C3b structure. The FI structure as well as the glycosylation sites (mutants and natural) is shown together with FH and C3b experimental structures (33). The core of the C3b structure is formed by eight macroglobulin (MGs) domains (shown in green and grey). Inserted between MG7 and MG8 is the CUB domain ('complement C1r-C1s, UEGF, BMP1') and a thioester containing domain (TED), which allows covalent attachment to target surfaces. The carboxyl terminus is extended by a C345C domain, which is common to complement components C3, C4 and C5. Only the four CCP domains of FH are shown (magenta). The model was generated as described previously (23). The C3b Arg1281 is positioned such as to fit into the catalytic site of the FI SP domain.

FIGURE 2. Identification of purified recombinant wt and extra N-glycosylated mutants. The purified proteins (0.1 μg/well) were separated by SDS-PAGE under non-reducing conditions and transferred to polyvinylidene difluoride membranes. The FI protein was detected using polyclonal goat anti-human FI ad polyclonal rabbit anti-goat antibody conjugated to horseradish peroxidase.

FIGURE 3. Degradation in the fluid phase of C3b and C4b by FI wt and mutants in the presence of FH and C4BP as cofactors. A and C. Recombinant wt or mutant FI (10 μg/ml) was incubated with C3met (A) or C4met (C), FH (A) or C4BP (C), and trace amounts of ^{125}I-C3b (A) or ^{125}I-C4b (C) for 90 min at 37°C and the separated on a 10-15% gradient SDS-PAGE. In the negative control (-ctrl) FI was omitted, and 20 μg/ml of FI was used as a positive control (+ctrl). Different degradation products are pointed with arrows. B and D. 10 μg/ml of the different types of FI were analyzed, and the generation of 43kDa or C4d products for C3b and C4d, respectively, were quantified by densitometry. The experiments were repeated three times, and the results are presented as % of the positive control present on each gel as means ± (standard deviation) S.D. One-way ANOVA with Tukey's multiple comparison tests were performed to evaluate the statistical significance of differences observed between wt and mutant FI. *, $p < 0.05$; **, $p < 0.01$; ***, $p < 0.001$.

FIGURE 4. Degradation in the fluid phase of C3b and C4b by FI wt and mutants in the presence of MCP and CR1 as cofactors. A and C. Recombinant wt or mutant FI (20 μg/ml) was incubated with C3met, MCP (A) or CR1 (C), and trace amounts of ^{125}I-C3b for 90 min at 37°C and the separated on a 10-15% gradient SDS-PAGE. In the negative control (-ctrl) FI was omitted, and 20 μg/ml of FI with 20 μg/ml FH was used as a positive control (+ctrl). Different degradation products are pointed with arrows. B and D. 20 μg/ml of the different types of FI were analyzed, and the generation of 43kDa product was quantified by densitometry. The experiments were repeated three times, and the results are presented as % of the positive control present on each gel as means ± S.D. One-way ANOVA with Tukey's multiple comparison tests were performed to evaluate the statistical significance of differences observed between wt and mutant FI. *, $p < 0.05$; **, $p < 0.01$; ***, $p < 0.001$.

FIGURE 5. Degradation of C3b by FI wt and mutants on surface. Sheep erythrocytes were opsonized with C3b by incubation with C3, FB and FD. Different concentrations of FI (0.1, 0.5 and 1 μg/ml) and 20 μg/ml FH were used to degrade C3b during incubation for 60 min at 37°C. The amounts of deposited C3b and formed iC3b were detected using specific monoclonal antibodies, and the results are presented as a ratio of iC3b:C3d. The experiments were repeated three times, and the means ± S.D. are shown. One-way ANOVA with Tukey's multiple comparison tests were performed to evaluate the statistical significance of differences observed between wt and mutant FI. *, $p < 0.05$; **, $p < 0.01$; ***, $p < 0.001$.

FIGURE 6. Analyses of the deglycosylation of wt FI and mutants. Mutants were incubated in native conditions with endoglycosidases for 24h at 37°C in a ratio enzyme:glycoprotein, 0.03 (v/w). Subsequently a fluid-phase degradation assay of all impaired mutants (5 and 10 μg/ml) with C3b and FH as cofactor was carried out. FI (20 μg/ml) was used as positive control. The experiments were repeated six times, and the results are shown as percentage of the positive control present on each gel as means ± S.D. Two-way ANOVA with Bonferroni post-tests were performed to evaluate the statistical significance of differences observed between wt and mutant FI. ***, $p < 0.001$.

FIGURE 7. Binding of wt and mutants FI to C3met or C4met. C3met or C4met was coated on microtiter plates and incubated with wt and mutant FI, and bond FI was detected with specific antibodies. Background signals originating from antibodies with empty well were substracted from the original values. Thus, the obtained values were normalized to the value obtained for the wt FI in each experiment. The experiments were repeated three times in duplicate, and ± S.D. are shown. One-way ANOVA with Tukey's multiple comparison tests were performed to evaluate the statistical significance of differences observed between wt and mutant FI. *, $p < 0.05$; **, $p < 0.01$; ***, $p < 0.001$.

TABLE 1
Primers used for site-directed mutagenesis
The mutations are marked in bold and underlined. In some cases more than one amino acid had to be altered to create consensus N-glycosylation site N-X-S/T.

Mutations[a]	Sequence (5' to 3')
R35N/I37T	GC CAG CCA TGG CAG A**AC** TGC A**C**T GAG GGC ACC TG
T54N/V56T	GC CCA AAG AAT GGC A**A**T GCA **AC**G TGT GCA ACT AAC AGG AG
R61N	CT GCA GTG TGT GCA ACT AAC A**AC** AGA AGC TTC CCA AC
F82N/N84T	CCA GGG ACA AAG **AA**T TTA A**C**T AAC GGA ACA TGC ACA GCC G
D104S	CC TTG AAG CAT GGA AAT ACA **AG**T TCA GAG GGA ATA G
K124N	CA ATG TTC ATA TGC AA**C** AGC AGC TGG AGC ATG AGG
L171N	CAT GTG CAT TGC CGA GGA **AAC** GAG ACC AGT TTG GCT G
K182N/R184S	GAA TGT ACT TTT ACT AA**C** AGA AG**C** ACT ATG GGT TAC CAG G
Q210N/V212T	CCA ATG GAT GAC TTC TTT **A**A**C** TGT GTG AAT GGG AAA TAC
Q219N/K221S	GTG AAT GGG AAA TAC ATT TCT **A**A**C** ATG A**GC** GCC TGT GAT GGT ATC
Q242N/K244S	CTG TGT TGT AAA GCA TGC **A**A**C** GGC A**GC** GGC TTC CAT TGC
Q257N/Q259S	GGT GTT TGC ATT CCA AGC **A**A**C** TAT **TC**A TGC TGC AAT GGT GAG G
K326N/A328T	GA ATT GTG GGA GGA AA**C** CGA **A**CA CAA CTG GGA GAC C
R365N	GCT CGA CAT TGT CTC A**AC** GCC AGT AAA ACT CAT CG
D385N/K387S	GTA GAC TGG ATA CAC CCC **A**AC CTT A**GC** CGT ATA GTA ATT G
N404T	C CAT GAA AAC TAC ACT GCA GGC A**C**T TAC CAA AAT G
D420N/N422T	G ATT GAA ATG AAA AAA **A**AC GGA A**C**C AAA AAA GAT TGT GAG CTG CC
K458N/N460T	GC TGG GGA CGA GAA AA**C** GAT A**C**C GAA AGA GTC TTT TC
D497N	GT GCA GGT ACA TAT **A**AT GGT TCC ATC GAT GCC
S561N/Y563T	GGA AGG CCT TTT ATT AAT CAG **AC**C AAT GTA TAA AAT TGT G

[a] Numbering without the signal peptide

TABLE 2
Kinetic parameters for DPR-AMC substrate cleavage by wt FI and the mutants

Mutations	n	V_{max}		K_m	
		Mean	**S.D.**	**Mean**	**S.D.**
wt	6	0.254	0.069	228.74 ***	51.76
R35N/I37T	6	0.332	0.063	67.31 ***	13.98
T54N/V56T	6	0.315	0.069	25.99 ***	4.74
R61N	6	0.276	0.044	89.06 ***	26.87
F82N/N84T	6	0.625 **	0.126	111.12	22.14
D104S	6	0.128	0.036	176.28	46.64
K124N	6	0.021	0.005	67.1 ***	22.85
L171N	6	0.236	0.118	95.62 ***	27.1
K182N/R184S	6	0.155	0.045	187.03	50.22
Q210N/V212T	6	0.095	0.035	133.86 **	27.44
Q219N/K221S	6	0.032	0.010	86.55 ***	18.84
Q242N/K244S	6	0.034	0.012	138.44 **	29.1
Q257N/Q259S	6	2.977 ***	0.565	69.82 ***	12.93
K326N/A328T	6	0.119	0.036	209.67	69.8
R365N	6	0.133	0.035	194.69	51.34
D385N/K387S	6	0.120	0.027	48.84 ***	13.59
N404T	6	0.189	0.056	155.68	33.14
D420N/N422T	6	0.187	0.062	140.04 *	19.82
K458N/N460T	6	0.179	0.046	206.49	69.91
D497N	6	0.146	0.049	134.21 **	30.72
S561N/Y563T	6	0.114	0.030	157.13	39.15

V_{max} is expressed as pmol of AMC released/min/mg of enzyme. K_m is expressed as mM.
The experiments were repeated three times. One-way ANOVA with Turkey's multiple comparison tests were performed to evaluate the statistical significance of differences observed between wt and mutant FI. ***, $p < 0.001$; **, $p<0.01$; *, $p<0.05$.

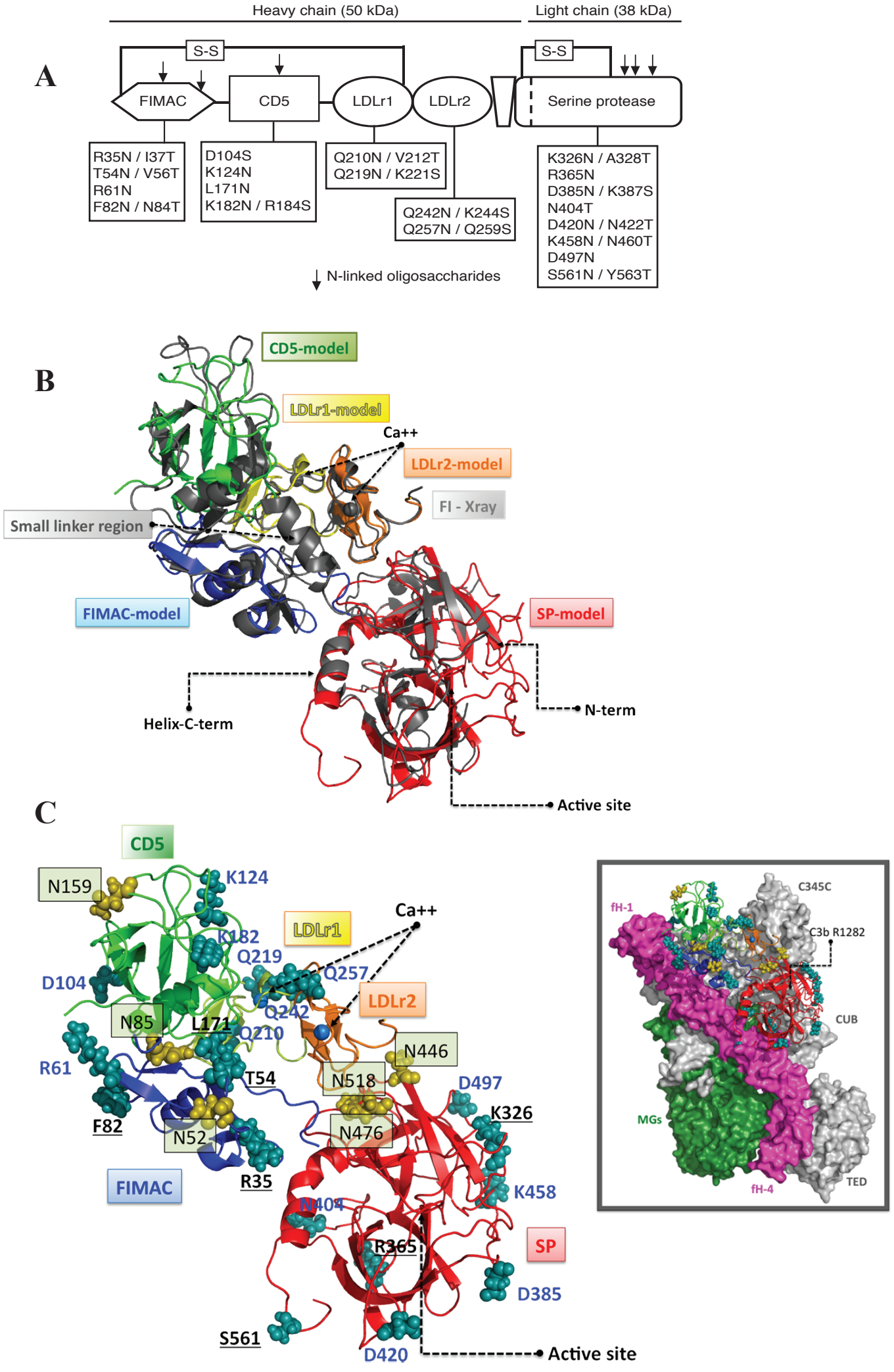
A
Heavy chain (50 kDa)
Light chain (38 kDa)
S-S
S-S
FIMAC
CD5
LDLr1
LDLr2
Serine protease
R35N / I37T
T54N / V56T
R61N
F82N / N84T
D104S
K124N
L171N
K182N / R184S
Q210N / V212T
Q219N / K221S
Q242N / K244S
Q257N / Q259S
K326N / A328T
R365N
D385N / K387S
N404T
D420N / N422T
K458N / N460T
D497N
S561N / Y563T
N-linked oligosaccharides
B
CD5-model
LDLr1-model
Ca++
LDLr2-model
FI - Xray
Small linker region
FIMAC-model
SP-model
Helix-C-term
N-term
Active site
C
CD5
N159
K124
Ca++
LDLr1
K182
Q219
Q257
D104
LDLr2
N85
L171
Q242
Q210
N446
R61
T54
N518
D497
K326
F82
N52
N476
FIMAC
R35
K458
N404
SP
R365
D385
S561
D420
Active site
fH-1
C345C
C3b R1282
CUB
MGs
fH-4
TED

Fig.2

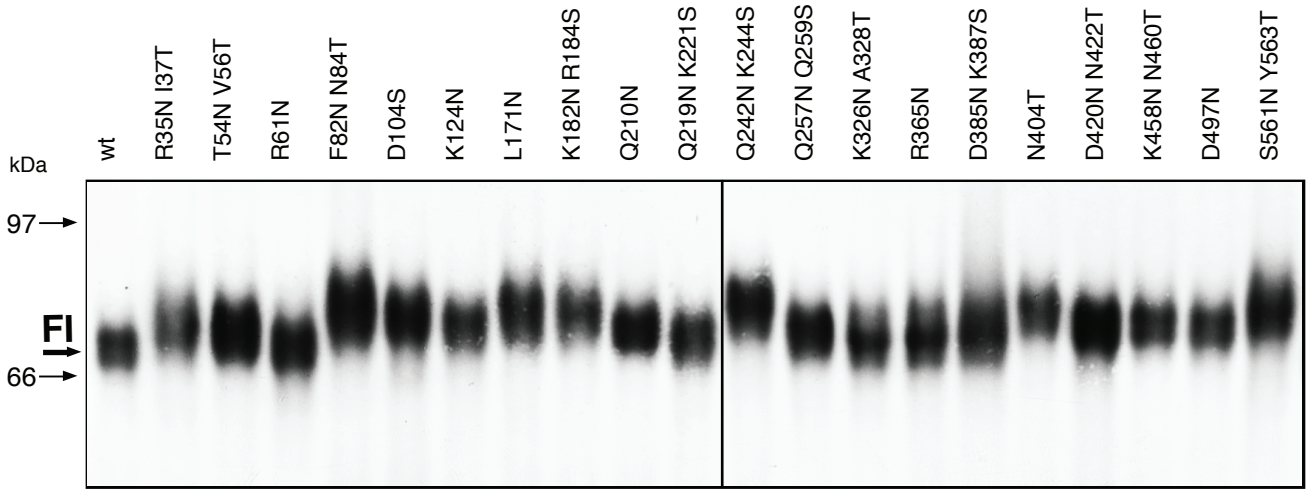
wt
R35N I37T
T54N V56T
R61N
F82N N84T
D104S
K124N
L171N
K182N R184S
Q210N
Q219N K221S
Q242N K244S
Q257N Q259S
K326N A328T
R365N
D385N K387S
N404T
D420N N422T
K458N N460T
D497N
S561N Y563T
kDa
97
FI
66

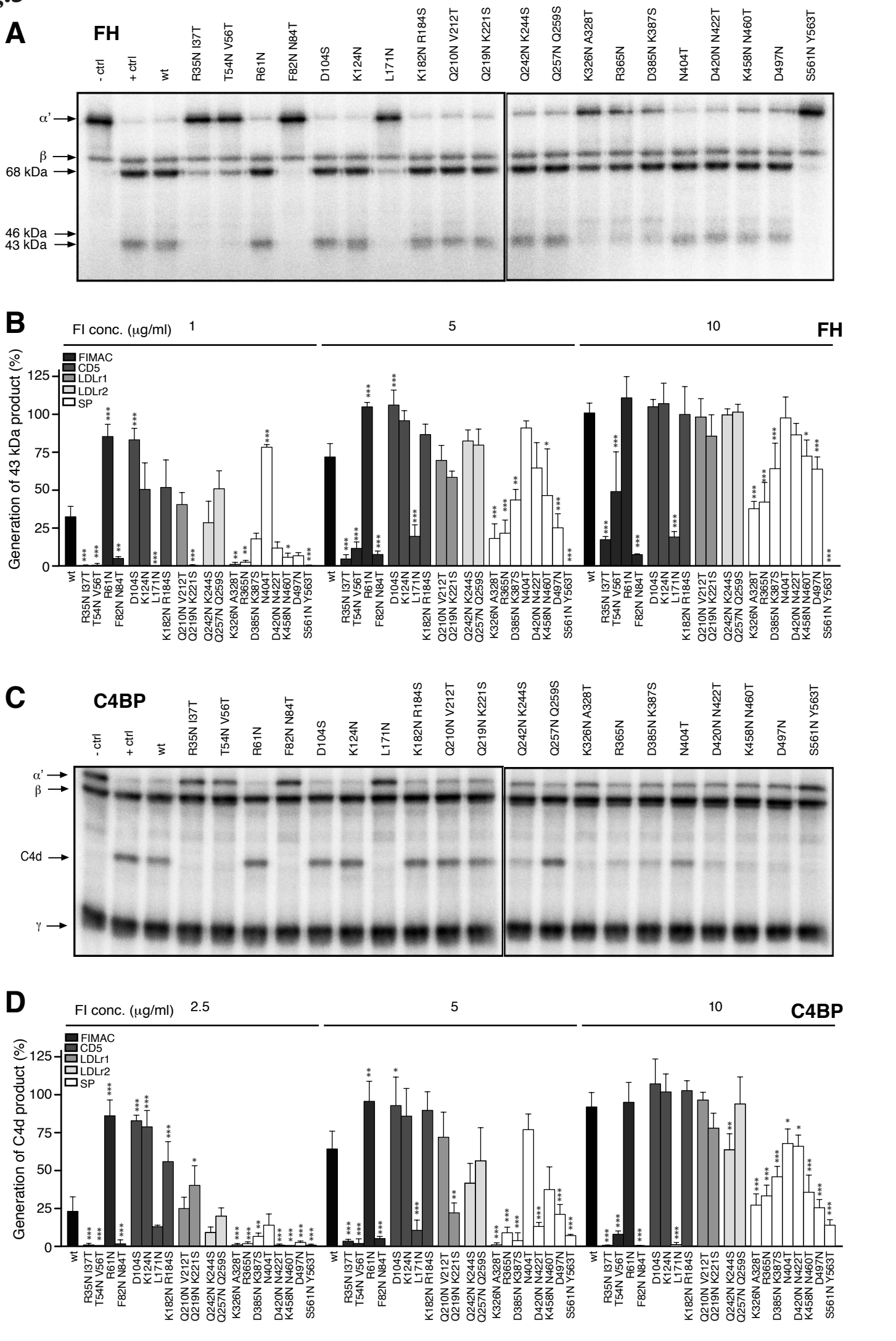
A
FH
- ctrl
+ ctrl
wt
R35N I37T
T54N V56T
R61N
F82N N84T
D104S
K124N
L171N
K182N R184S
Q210N V212T
Q219N K221S
Q242N K244S
Q257N Q259S
K326N A328T
R365N
D385N K387S
N404T
D420N N422T
K458N N460T
D497N
S561N Y563T
α'
β
68 kDa
46 kDa
43 kDa
B
FI conc. (μg/ml)
1
5
10
FH
FIMAC
CD5
LDLr1
LDLr2
SP
Generation of 43 kDa product (%)
125
100
75
50
25
0
wt
C
C4BP
C4d
γ
D
FI conc. (μg/ml)
2.5
5
10
C4BP
Generation of C4d product (%)

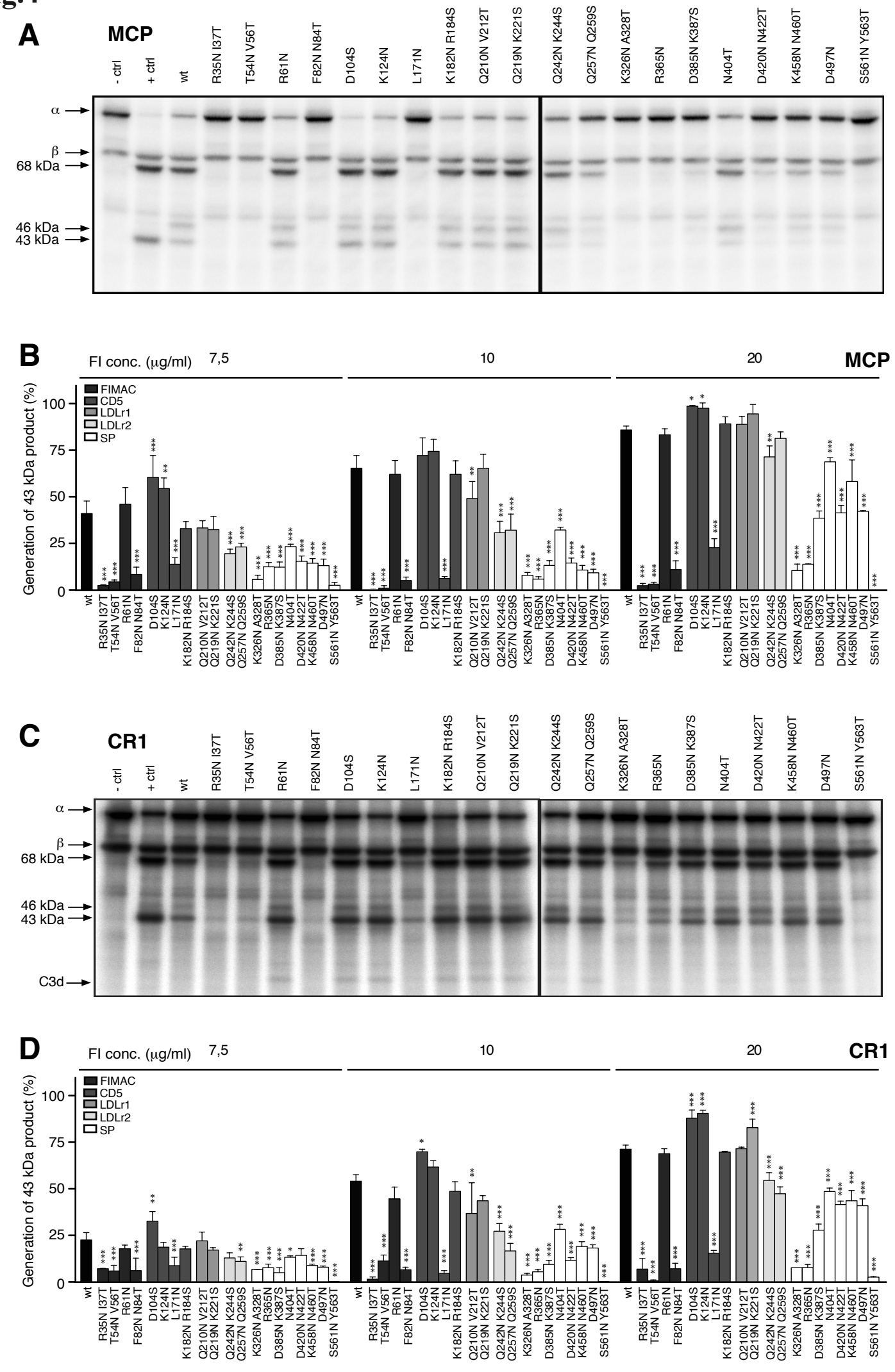
A
MCP
- ctrl
+ ctrl
wt
R35N I37T
T54N V56T
R61N
F82N N84T
D104S
K124N
L171N
K182N R184S
Q210N V212T
Q219N K221S
Q242N K244S
Q257N Q259S
K326N A328T
R365N
D385N K387S
N404T
D420N N422T
K458N N460T
D497N
S561N Y563T
α
β
68 kDa
46 kDa
43 kDa
B
FI conc. (μg/ml)
7,5
10
20
MCP
Generation of 43 kDa product (%)
FIMAC
CD5
LDLr1
LDLr2
SP
C
CR1
C3d
D
FI conc. (μg/ml)
7,5
10
20
CR1
Generation of 43 kDa product (%)
FIMAC
CD5
LDLr1
LDLr2
SP

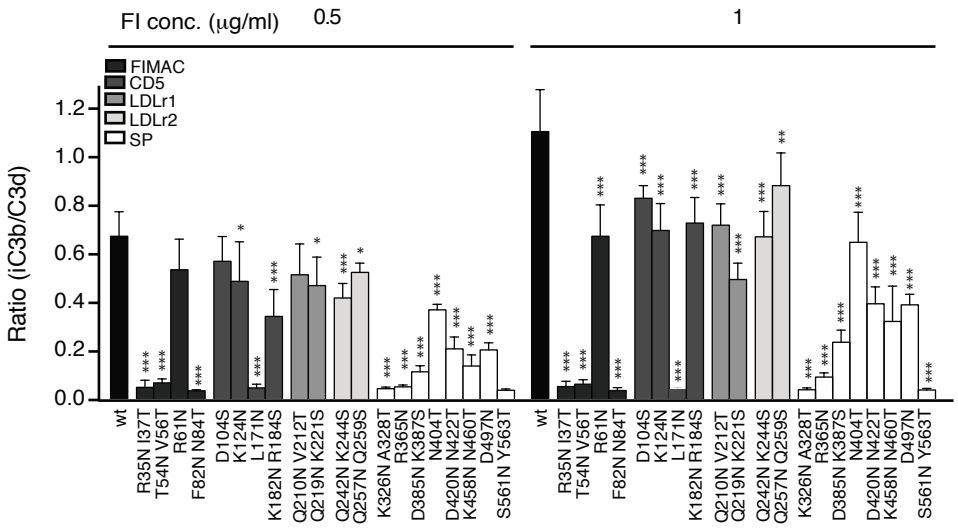
FI conc. (μg/ml)
0.5
1
FIMAC
CD5
LDLr1
LDLr2
SP
Ratio (iC3b/C3d)
0.0
0.2
0.4
0.6
0.8
1.0
1.2
wt
R35N I37T
T54N V56T
R61N
F82N N84T
D104S
K124N
L171N
K182N R184S
Q210N V212T
Q219N K221S
Q242N K244S
Q257N Q259S
K326N A328T
R365N
D385N K387S
N404T
D420N N422T
K458N N460T
D497N
S561N Y563T

Fig.6

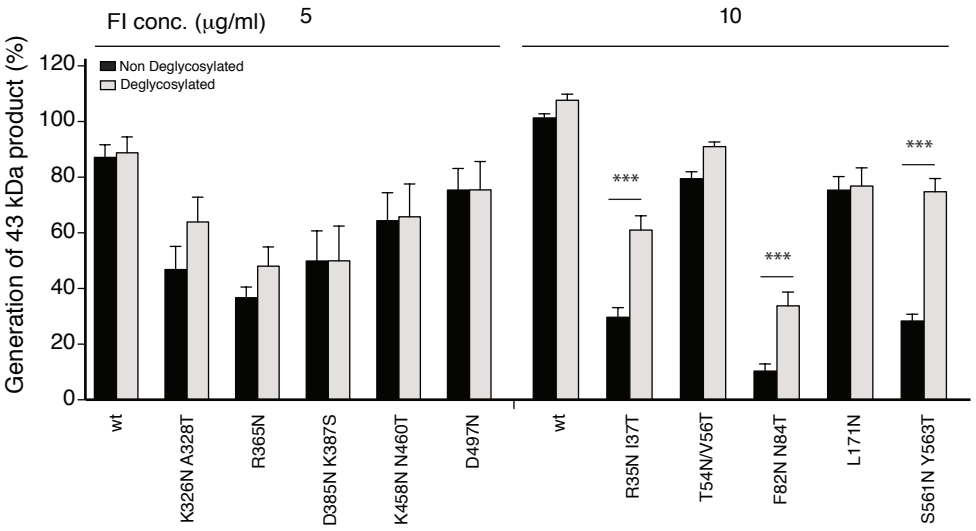
FI conc. (μg/ml)
5
10
Non Deglycosylated
Deglycosylated
Generation of 43 kDa product (%)
120
100
80
60
40
20
0
***
***
***
wt
K326N A328T
R365N
D385N K387S
K458N N460T
D497N
wt
R35N I37T
T54N/V56T
F82N N84T
L171N
S561N Y563T

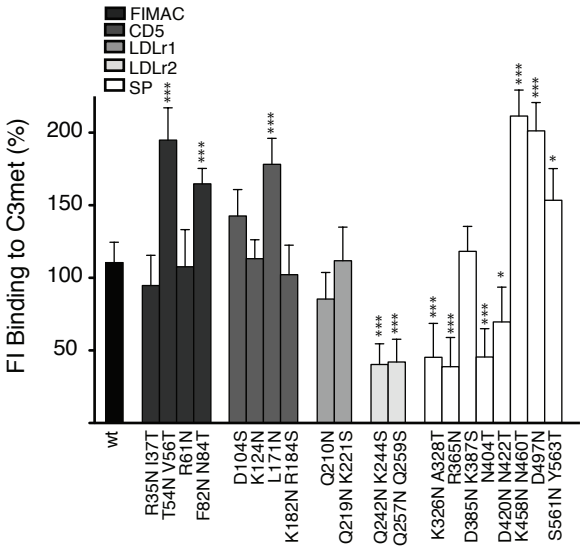
FIMAC
CD5
LDLr1
LDLr2
SP
FI Binding to C3met (%)
200
150
100
50
wt
R35N I37T
T54N V56T
R61N
F82N N84T
D104S
K124N
L171N
K182N R184S
Q210N
Q219N K221S
Q242N K244S
Q257N Q259S
K326N A328T
R365N
D385N K387S
N404T
D420N N422T
K458N N460T
D497N
S561N Y563T

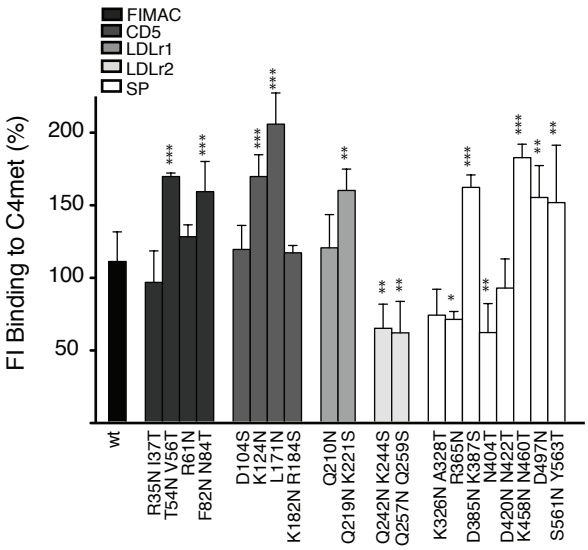
FIMAC
CD5
LDLr1
LDLr2
SP
FI Binding to C4met (%)
200
150
100
50
wt
R35N I37T
T54N V56T
R61N
F82N N84T
D104S
K124N
L171N
K182N R184S
Q210N
Q219N K221S
Q242N K244S
Q257N Q259S
K326N A328T
R365N
D385N K387S
N404T
D420N N422T
K458N N460T
D497N
S561N Y563T